# An Improved Mach-Box Approach for Supersonic Oscillatory Pressures

Richard R. Chipman*
*Grumman Aerospace Corporation, Bethpage, N. Y.*

**An analytical refinement of the Mach-box approach has been developed which provides greatly improved supersonic oscillatory pressure distributions with almost no increase in computer time over that required by the original formulation. The refinement consists, in part, of applying physically justifiable weighting factors to the terms of the aerodynamic influence coefficient matrix. Unlike approaches that employ curve smoothing to eliminate the erratic undulations in computed pressures obtained by the basic method, the present analysis produces well-behaved pressure distributions while retaining essential flow discontinuities. Furthermore, the present method is more cost-effective than approaches relying on refinements in the aerodynamic grid to obtain comparable improvements in the calculated pressures.**

## Nomenclature

$A$ = area of an aerodynamic element or box representing part of a lifting surface or diaphragm
$b$ = streamwise dimension of a box, or semispan of a wing if indicated
$c$ = local chord
$\bar{c}$ = mean chord
$c_l$ = local lift coefficient
$C_L$ = total lift coefficient
$C_j$ = influence coefficient relating the pressure at a point due to a unit downward over the $j$th box
$C_{MN}$ = influence coefficient relating the pressure at a type $M$ point due to a unit downwash over a type $N$ box, where $M$ and $N$ may be $W$, $D$, $WS$, or $DS$
$\Delta\bar{C}_P$ = amplitude of the lifting pressure at a point
$\Delta\bar{C}_{P,M}$ = amplitude of the lifting pressure at a type $M$ point
$k$ = reduced frequency $= b\omega/U$
$\tilde{k}$ = transformed reduced frequency $= (M/\beta)^2 k$
$M$ = Mach number
$R$ = hyperbolic radius $= \sqrt{(x-\zeta)^2 - \beta^2(y-\eta)^2}$
$\tilde{R}$ = transformed hyperbolic radius $= \sqrt{(\tilde{x}-\tilde{\zeta})^2 - (\tilde{y}-\tilde{\eta})^2}$
$S$ = area of integration bounded by the forward-facing Mach cone emanating from $(x,y)$ and by either the planform leading edge or the most forward rearward-facing cone emanating from the planform apex, whichever is most forward
$t$ = time
$U$ = freestream velocity
$\bar{W}$ = amplitude of the downwash
$\bar{W}_M$ = amplitude of the downwash over a type $M$ box
$x,y,z$ = streamwise, lateral, and vertical coordinates
$\tilde{x},\tilde{y}$ = defined in Eq. (4)
[AIC] = aerodynamic influence coefficient matrix
$AR$ = aspect ratio
$\alpha$ = angle of attack
$\beta$ = $\sqrt{M^2-1}$
$\zeta,\eta$ = streamwise and lateral dummy variables
$\tilde{\zeta},\tilde{\eta}$ = defined in Eq. (4)
$\Lambda$ = sweep angle of planform leading edge
$\phi$ = perturbation velocity potential
$\omega$ = radial frequency of oscillation of the surface displacement and, hence, of the downwash and pressure distributions
$\bar{\omega}$ = $\omega M^2/U\beta^2$

*Subscripts*

$D$ = diaphragm box
$DS$ = diaphragm portion of a shared box
$W$ = lifting surface (wing) box
$WS$ = surface portion of a shared box
$j$ = box index

Presented at the AIAA/ASME/SAE 17th Structures, Structural Dynamics, and Materials Conference, King of Prussia, Pa., May 5-7, 1976 (in bound volume of Conference papers, no paper number); submitted May 7, 1976; revision received April 27, 1977.

Index categories: Nonsteady Aerodynamics; Supersonic and Hypersonic Flow.

*Senior Aeroelasticity Engineer. Member AIAA.

## Introduction

SINCE its initial development by Pines et al.,[1] the pressure influence coefficient (PIC) method, when implemented with a box approach, has been the most widely employed technique for the computation of oscillatory aerodynamic loads for inviscid supersonic flow. The kernel function techniques of Watkins and Berman[2] and Cunningham[3] are less general, require user knowledge of the characteristics of the solution, and consequently have received less usage. Other recently developed approaches, such as Brock and Griffin's supersonic doublet-lattice method[4] and Giesing and Kalman's finite-element doubled method,[5] possess great generality and will be invaluable, when extended, in treating complex wing-body configurations; however, they require significantly more computing time than the PIC box method.

Because usage of the PIC box approach has been and will continue to be substantial, it is appropriate to attempt to remedy one conspicuous shortcoming, namely, the erratic undulations in the computed pressures that have plagued this method since its inception. In fact, were it not true that the basic method produces useable generalized force for elementary mode shapes regardless of the erratic pressure distributions, development and use of this method certainly would have been abandoned. The present paper describes and demonstrates a method of modifying the Mach-box approach to produce well-behaved pressures without sacrificing its basic computational efficiency. Previous efforts at achieving the same improvement also are discussed.

## Theory

### Basic Linearized Supersonic Theory

The linearized perturbation potential equation for supersonic flow is

$$(1-M^2)\phi_{xx} + \phi_{yy} + \phi_{zz} - (2M^2/U)\phi_{xt} - (M^2/U^2)\phi_{tt} = 0 \quad (1)$$

Supersonic flow over a thin lifting surface at small incidence must satisfy this equation and the boundary condition obtained by assuming that the flow is tangential to the instantaneous position of the surface. For a planar surface undergoing small harmonic oscillations at a radial frequency $\omega$, the solution of Eq. (1) can be shown[6] to be

$$\phi(x,y,t) = -\frac{e^{i\omega t}}{\pi}\int\int_S \bar{W}(x,y)\cdot\exp[-i\bar{\omega}(x-\zeta)]\cdot\cos\left(\frac{\omega R}{M}\right)\cdot\frac{d\zeta d\eta}{R} \quad (2)$$

Using the linearized expression for the local differential (or lifting) pressure coefficient $\Delta C_P$, the complex amplitude of the pressure coefficient can be expressed as

$$\Delta\bar{C}_P = -\frac{4}{\pi}\left(\frac{\partial}{\partial x}+\frac{i\omega}{U}\right) \times\int\int_S \frac{\bar{W}}{U}\cdot\exp[-i\bar{\omega}(x-\zeta)]\cdot\cos\left(\frac{\bar{\omega}R}{M}\right)\frac{d\zeta d\eta}{R} \quad (3)$$

Using this equation, the pressure can be determined at any point in the plane of the planform once the downwash has been specified over $S$.

The downwash is determined at all points on the planform; but, since region $S$ also includes, in general, points not on the planform, an additional relationship must be used to determine the downwash at such points. Evvard[7] named the region comprised of these points the "diaphragm" and recognized that the required extra relationship is that the differential pressure in this region must be identically zero. Because this is so, Eq. (3), with its left-hand side set to zero, may be applied at such points and solved inversely for the required downwash distribution. More will be said about this scheme below.

### Mach-Box Technique

Because of its complexity, the integral in Eq. (3) cannot be evaluated analytically but must be treated numerically. Following the basic approach of Pines et al.,[1] the given planform is divided into small rectangular boxes, as shown in Fig. 1. Using the modifications of Zartarian and Zsu,[8] the boxes are sized such that their diagonals are aligned with the Mach lines. Then the boxes are converted to squares by the coordinate transformations

$$\bar{x}=x/b \qquad \bar{\xi}=\xi/b$$

$$\bar{y}=\beta y/b \qquad \bar{\eta}=\beta\eta/b \quad (4)$$

A critical simplification now is made by assuming that the downwash is constant over each of these "Mach boxes." With this simplification, Eq. (3) becomes

$$\Delta\bar{C}_p(\bar{x},\bar{y}) = \frac{-4}{\beta\pi}\sum_j \bar{w}_j\left(\frac{\partial}{\partial\bar{x}}+ik\right) \cdot\int\int_{S_j} e^{-ik(\bar{x}-\bar{\xi})}\cdot\cos\frac{k\bar{R}}{M}\cdot\frac{d\bar{\xi}d\bar{\eta}}{\bar{R}} \quad (5)$$

or

$$\bar{C}_p(\bar{x},\bar{y}) = \sum_j \bar{w}_j C_j(\bar{x},\bar{y}) \quad (6)$$

Two methods classically have been used to perform the complex integration over the box area. The first, developed in Ref. 1, uses a mean value of the exponential and cosine terms when a box is far removed from the point $(\bar{x},\bar{y})$ and a series expansion up to $k^2$ when a box is close. Although these approximations simplify the integration, they introduce significant errors when the reduced frequency $k$ is high. For a more exact evaluation, a second method, a Bessel function series representation of the integral, is presented in Ref. 8.

The method used in the current work is different from both of these methods in that weighted Gaussian quadrature (Ref. 9, p. 327 ff.) is used to evaluate the integral. With this technique, singularities that occur in the integrand when the box area is cut or touched by the inverse Mach cone emanating from the point $(\bar{x},\bar{y})$ can be accounted for accurately.

Equations (5) and (6) imply that, at a given Mach number and reduced frequency, the pressure influence coefficients are functions of only the separation, in units of box width, between the sending and receiving box centers in the streamwise and lateral directions (denoted, say, by $l$ and $m$, respectively). Consequently, influence coefficients need be computed only once for each admissable $l,m$ pair ($l\geq 0$, $0\leq m\leq l$) and can be summed appropriately via Eq. (6) when needed.

### Treatment of Subsonic Edges (Original Method)

The pressure on any box is a function of the downwash of only those boxes within the inverse Mach cone emanating from its box center. For a surface, the edges of which are all supersonic, the pressure is, furthermore, influenced only by boxes on the planform. If any of the surface edges are subsonic, however, there are regions adjacent to these edges which do affect the pressure on some areas of the planform. To account for this effect, the concept of a permeable "diaphragm" is introduced as discussed previously. This permeable sheet is bounded by the surface edge and the Mach lines emanating from the corners of the lifting surface and is represented by boxes in the same manner as the wing (Fig. 1).

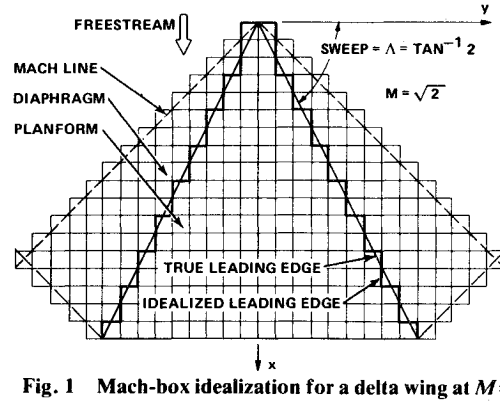


**Fig. 1 Mach-box idealization for a delta wing at $M=\sqrt{2}$.**

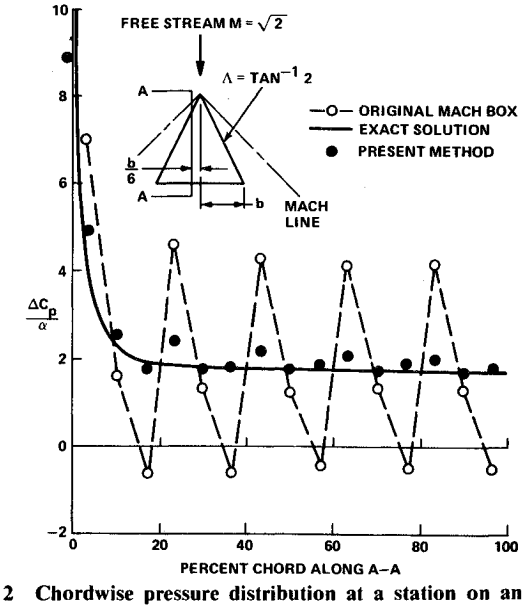


**Fig. 2 Chordwise pressure distribution at a station on an aspect-ratio-2 delta wing at steady-state angle of attack.**

In the original approaches of Refs. 1 and 8, boxes cut by the planform leading edge are designated as either wing or diaphragm boxes, depending on whether or not the box center lies on or off the wing. The relationship between the pressure coefficients and the downwash of the boxes on the combined wing and diaphragm can be written as

$$\begin{Bmatrix} \Delta\bar{C}_{P,W} \\ \hline \Delta\bar{C}_{P,D} \end{Bmatrix} = \left[\begin{array}{c|c} [C_{WW}] & [C_{WD}] \\ \hline [C_{DW}] & [C_{DD}] \end{array}\right] \begin{Bmatrix} \bar{W}_W \\ \hline \bar{W}_D \end{Bmatrix} \tag{7}$$

Since the pressure on any diaphragm box is zero, the unknown diaphragm downwash can be evaluated by

$$\{\bar{w}_D\} = -[C_{DD}]^{-1}[C_{DW}]\{\bar{w}_W\} \tag{8}$$

Substituting this result into Eq. (7) yields the final expression for the pressures on the wing boxes:

$$\{\Delta\bar{C}_{P,W}\} = [[C_{WW}] - [C_{WD}][C_{DD}]^{-1}[C_{DW}]]\{\bar{w}_W\}$$

$$= [\mathrm{AIC}]\{\bar{w}_W\} \tag{9}$$

When this formulation is used, the irregularity of the leading-edge representation leads to erratic pressure distributions. In Fig. 2, the open circles show pressures computed by the foregoing method for the delta wing shown in Fig. 1 at angle of attack. The results fluctuate greatly about the exact conical-flow solution.

**Alternate Methods**

Various techniques have been attempted to reduce these fluctuations in the pressure distributions. For example, some improvement can be obtained first by solving Eq. (2) for the velocity potential using the box approach and then performing streamwise differentiation by a numerical differencing scheme to obtain the pressures. Optionally, the velocity potential can be smoothed (by a least-square fit, for example) before the numerical differentiation is performed. Both Andrew and Moore[10] and Ii[11,17] have employed these techniques; but, as Ii points out, the smoothing method can lead to significant error for complex modes and high reduced frequencies. Not mentioned by Ii, but equally important, is the fact that smoothing will tend to eliminate theoretically correct pressure discontinuities that can occur in supersonic flow.

If one is willing to sacrifice computational speed, a grid-refinement method, in which a finer-box grid is used to model signal-sending regions than is used to define signal-receiving points, can be employed. Whereas a simple refinement of both sending and receiving boxes does not reduce the amplitude of the fluctuations, the refinement of only the sending boxes has proven to lead to a much smoother pressure distribution.[11] Since influence coefficients must be computed for every combination of streamwise and lateral separation $(l,m)$, the use of this or any grid-refinement scheme greatly increased the computational time required; hence, this approach becomes very costly for routine calculations.

Suggested in Ref. 10 is a technique to compute the source strength on each leading-edge box as the weighted average of the value it would assume if it were completely on the surface and that value it would assume if it were completely in the diaphragm. The weighting factors are the box areas on the planform and on the diaphragm, respectively. This method, when used together with the smoothing technique, does rid the pressure distribution of oscillations, but, as mentioned previously, the smoothing process introduces other accuracy problems. Another area-weighting scheme was used by Li,[18] but, since computed pressure distributions do not seem to have been published, an assessment of its success is not available.

**Present Method**

The method employs Li's and Andrew's concept of area-weighted wing and diaphragm boxes but does not average them and does not employ smoothing; furthermore, the pressures are computed directly (analytically), not by differencing. In this method, any box that is crossed by a planform edge is considered to consist of two identical overlapping boxes, one being treated as if it were on the planform and the other as if it were on the diaphragm. The pressures, downwashes, and influence coefficients for such boxes will be denoted by the subscripts $WS$ (wing, shared) and $DS$ (diaphragm, shared) in what follows.

Next, since the area of the planform encaptured by a box $WS_i$ is only a fraction, $A_{WS_i}/A$, of the full box area (see Fig. 3a), the contribution to the pressure at any other box due to a signal originating from this box should be scaled by roughly this ratio. Similarly, signals from a box $DS_i$ should be ratioed by

$$A_{DS_i}/A = 1 - A_{WS_i}/A$$

Incorporating these ideas, Eq. (7) becomes

$$\begin{Bmatrix} \Delta\bar{C}_{P,W} \\ \hline \Delta\bar{C}_{P,WS} \\ \hline \Delta\bar{C}_{P,DS} \\ \hline \Delta\bar{C}_{P,D} \end{Bmatrix} = \left[\begin{array}{c|c|c|c} [C_{WW}] & [C_{WWS}]\cdot[A_{WS}] & 0 & [C_{WD}] \\ \hline [C_{WSW}] & [C_{WSWS}]\cdot[A_{WS}] & 0 & [C_{WSD}] \\ \hline [C_{DSW}] & 0 & [C_{DSDS}]\cdot[A_{DS}] & [C_{DSD}] \\ \hline [C_{DW}] & 0 & [C_{DDS}]\cdot[A_{DS}] & [C_{DD}] \end{array}\right] \begin{Bmatrix} \bar{W}_W \\ \hline \bar{W}_{WS} \\ \hline \bar{W}_{DS} \\ \hline \bar{W}_D \end{Bmatrix} \tag{10}$$

where the factors of $1/A$ are omitted, since the area of a full box in the transformed Mach-box system is identically unity.

The zero submatrices in the influence coefficient array are necessary to permit realistic nonzero pressures on the shared boxes. For example, consider the apex box of a wing with subsonic edges. No other box on the surface affects this box, since all others are downstream. Therefore, if the indicated submatrices were not zero, the portion of Eq. (10) pertaining to the apex box would read

$$\begin{Bmatrix} \Delta\bar{C}_{P_1} \\ \hline 0 \end{Bmatrix} = \left[\begin{array}{c|c} C_{11}A_1 & C_{11}(1-A_1) \\ \hline C_{11}A_1 & C_{11}(1-A_1) \end{array}\right] \begin{Bmatrix} W_{W_1} \\ \hline W_{D_1} \end{Bmatrix} \tag{11}$$

and, hence, the pressure on the box would be

$$\Delta\bar{C}_{P_1} = C_{11}[A_1 W_{W_1} + (1-A_1)W_{D_1}]$$

$$= C_{11}\{A_1 - (1-A_1)[A_1/(1-A_1)]\}W_{W_1} \equiv 0 \tag{12}$$

On the other hand, in the present method the two off-diagonal coefficients in Eq. (11) are zero, and the pressure $\Delta\bar{C}_{P_1}$ becomes that of a nonshared surface box.

Analogous to Eq. (7), Eq. (10) is solved first for $\{W_{DS}\}$ and $\{W_D\}$ by setting $\{\Delta\bar{C}_{P,DS}\}$ and $\{\Delta\bar{C}_{P,D}\} = 0$. This yields an equation comparable to Eq. (8). Then a final expression for the pressures on the surface is obtained comparable to Eq. (9). It should be noted that

$$[C_{WSW}] \equiv [C_{DSW}], [C_{WSD}] \equiv [C_{DSD}], [C_{WSWS}] \equiv [C_{DSDS}]$$

because the shared box $WS_i$ is located coincident with the box $DS_i$. Consequently, no additional influence coefficients must be computed; those obtained for the basic method are used

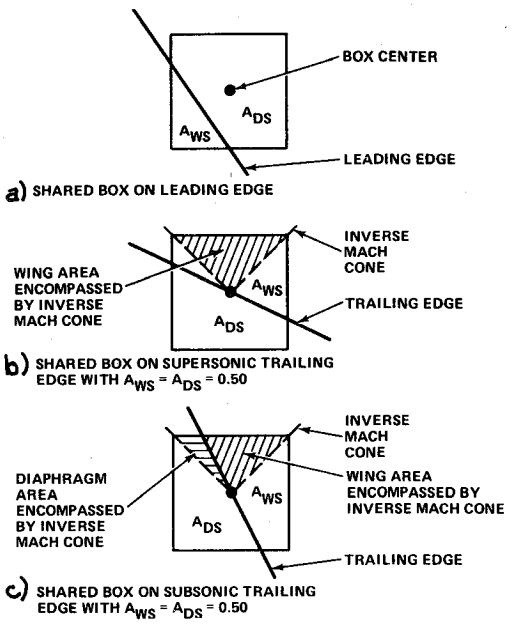


Fig. 3 Geometry for representative shared boxes.

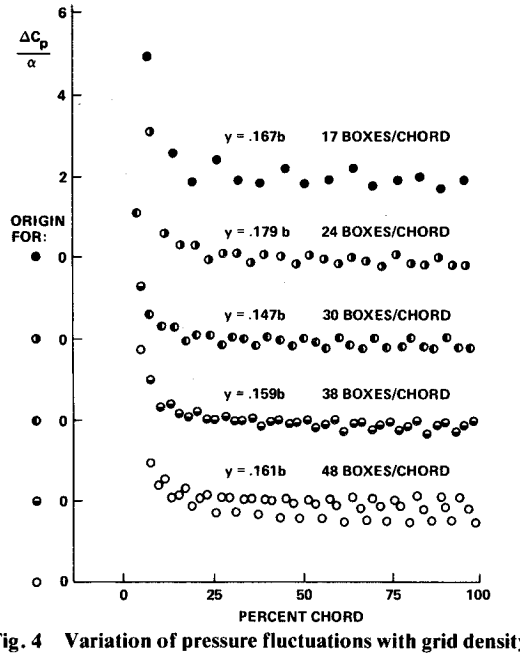


Fig. 4 Variation of pressure fluctuations with grid density.

with at most an area ratio to be applied. Hence, the computational time is increased only slightly.

In the case where all planform edges are supersonic. no diaphragm exists, and Eq. (10) reduces to

$$\begin{Bmatrix} \Delta\bar{C}_{P,W} \\ \Delta\bar{C}_{P,WS} \end{Bmatrix} = \begin{bmatrix} [C_{WW}] & [C_{WWS}]\cdot[A_{WS}] \\ [C_{WSW}] & [C_{WSWS}]\cdot[A_{WS}] \end{bmatrix} \begin{Bmatrix} \bar{W}_W \\ \bar{W}_{WS} \end{Bmatrix} \tag{13}$$

Since the area of the planform covered by each leading-edge box is still only a fraction of a full box area, the scaling is retained in this case as well, and such boxes still are denoted by the subscript $WS$ even though they are not "shared" with a diaphragm box.

Results obtained by the preceding formulation require some interpretation. Because of the jagged representation of the leading edge, the centers of some shared boxes may lie physically ahead of the true planform (see Fig. 3a); yet, nonzero pressures are computed for such boxes. This is acceptable, since the calculated pressure coefficient $\Delta\bar{C}_{P,WS}$ is applied over the entire box area, and, certainly, the pressure over $A_{WS}$ is nonzero. Now, if the force $\Delta\bar{C}_{P,WS}\cdot A$ is applied to only the correct area $A_{WS}$, the true pressure coefficient for that area would be $(\Delta\bar{C}_{P,WS}\cdot A)/A_{WS}$ or, since $A=1$, $\Delta\bar{C}_{P,WS}/A_{WS}$. However, since the contribution from such shared boxes to the generalized force is given by

$$Q = ([A_{WS}]\cdot\{\Delta\bar{C}_{P,WS}/A_{WS}\})^T\cdot\{h_{WS}\}$$

$$= \{\Delta\bar{C}_{P,WS}\}^T\cdot\{h_{WS}\} \tag{14}$$

the pressures computed by Eq. (10) rather than the weighted values actually are used in the computer program.

In Fig. 2, the pressure distribution computed by the preceding formulation, with the weighting factor $1/A_{WS}$ applied to the leading-edge boxes, is indicated by the solid circles. A substantial improvement is apparent over the entire chord.

A small change in the preceding formulation has been found to improve the smoothness slightly. The modification consists of not including the area weights on the diaphragm boxes. Equation (10) then becomes

$$\begin{Bmatrix} \Delta\bar{C}_{P,W} \\ \Delta\bar{C}_{P,WS} \\ \Delta\bar{C}_{P,DS} \\ \Delta\bar{C}_{P,D} \end{Bmatrix} = \begin{bmatrix} [C_{WW}] & [C_{WWS}]\cdot[A_{WS}] & 0 & [C_{WD}] \\ [C_{WSW}] & [C_{WSWS}]\cdot[A_{WS}] & 0 & [C_{WSD}] \\ [C_{DSW}] & 0 & [C_{DSDS}] & [C_{DSD}] \\ [C_{DW}] & 0 & [C_{DDS}] & [C_{DD}] \end{bmatrix} \begin{Bmatrix} \bar{W}_W \\ \bar{W}_{WS} \\ \bar{W}_{DS} \\ \bar{W}_D \end{Bmatrix} \tag{15}$$

One additional set of refinements is necessary to handle trailing edges properly. On an average, a box cut by a trailing edge will have 50% of its area on the wing and 50% behind the wing. For such a case, when the edge is supersonic, the inverse Mach cone from a point at the center of the box encompasses the same wing area, $A/4$, as does any upstream whole wing box (see Fig. 3b). Furthermore, for a trailing-edge box, the influence of a box on itself is almost the only significant consideration, whereas, for any other type of box, the effect of that box on other aft boxes also is significant. Therefore, for a shared box on a supersonic trailing edge, the area ratio used elsewhere is not applied; i.e., the influence coefficient is $C_{WSWS}$, not $C_{WSWS}\cdot A_{WS}$.

The case of a box on a subsonic trailing edge is only slightly different (see Fig. 3c). The wing area encompassed by the inverse Mach cone is still generally a much larger percentage of the total Mach cone area than is indicated by the value of $A_{WS}$. Therefore, in this case also the influence coefficient is not scaled.

It should be noted that, when the factor $A_{WS}$ is omitted from the influence-coefficient calculation, the reciprocal factor $1/A_{WS}$ is omitted from the pressure calculation. However, the generalized-force contribution for a trailing-edge box still is scaled by the factor $A_{WS}$.

The computations previously shown (Fig. 2) were for planforms with supersonic trailing edges and were made including the foregoing refinements. Demonstrations for a subsonic trailing edge are presented later.

### Grid Selection

Although use of the present method greatly reduces the oscillations in the pressure distributions which were apparent in the basic method, some fluctuations do remain. The use of

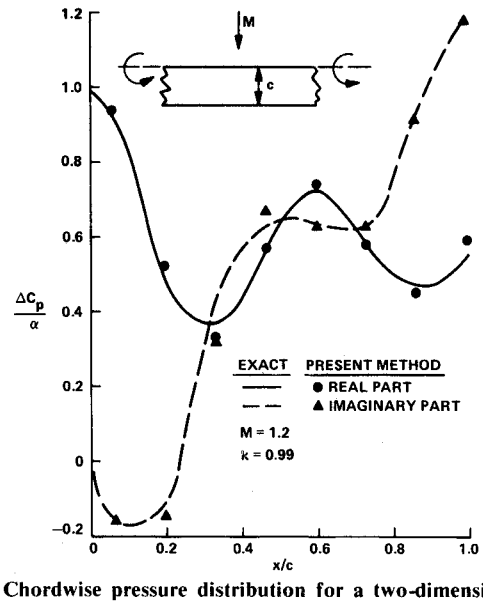


Fig. 5 Chordwise pressure distribution for a two-dimensional unswept wing oscillating in pitch at $k = 0.99$.

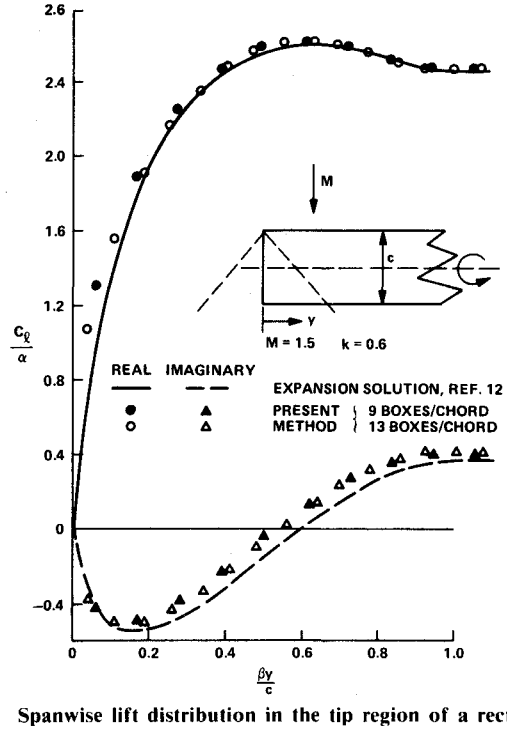


Fig. 6 Spanwise lift distribution in the tip region of a rectangular wing oscillating in pitch.

a finer grid is, of course, no panacea for this problem and, in fact, can worsen the computations. Figure 4 shows the pressure distribution at a spanwise station on the previously treated aspect-ratio-2 delta wing for various grid densities. Some improvement is realized by increasing the number of boxes from 80 to 200 on the planform (17 to 24 on the chord), but the fluctuations grow noticeably larger in going from 200 to 800 boxes on the planform. Hence, some "tuning" should be performed to select the proper grid density for a particular planform.

## Results

To evaluate further the present method's accuracy, pressures were computed on several planforms for both steady and oscillatory conditions. The results are compared with available exact solutions or with the results of other theoretical methods.

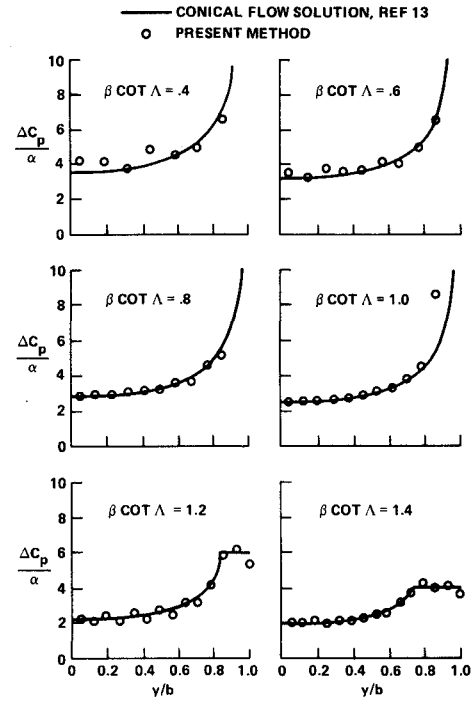


Fig. 7 Spanwise pressure distributions at midchord of delta wing, $\mathcal{R} = 4$, at steady-state angle of attack.

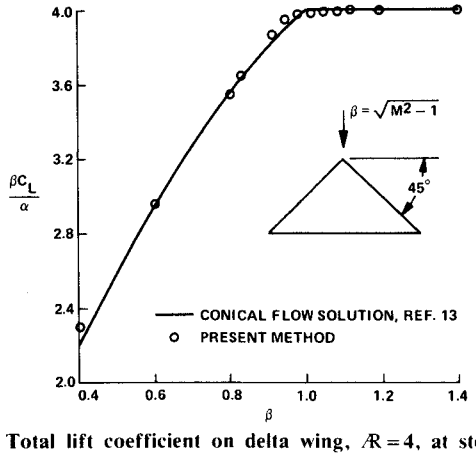


Fig. 8 Total lift coefficient on delta wing, $\mathcal{R} = 4$, at steady-state angle of attack.

Figure 5 presents pressures inboard of the tip effect on a high-aspect-ratio rectangular wing at $M = 1.2$ oscillating in pitch about its leading edge at a reduced frequency of $k = 0.99$. As expected for this simple case, agreement between results of the present method and the exact two-dimensional solution is excellent. For this wing pitching about its midchord at $k = 0.6$ and $M = 1.5$, Fig. 6 presents the spanwise loading near the wingtip. Correlation with an expansion solution [12] is good and improves slightly with the use of a finer grid.

For an aspect-ratio-4 delta wing at a steady-state angle of attack, pressures were computed over a range of Mach numbers, such that $\beta \cos\Lambda$ varied from 0.4 to 1.4. The resulting spanwise lift distributions and the total lift coefficients are compared in Figs. 7 and 8 with the exact conical flow solutions. [13] Although agreement is good in all cases, it is worse at the lowest Mach number. Since this case corresponds to a Mach number (1.077) below the generally accepted limits of applicability of linearized aerodynamics, this failing is not considered serious.

For a 60 deg swept delta wing at $M = 1.436$ pitching about its root midchord at a reduced frequency of 0.74, Fig. 9

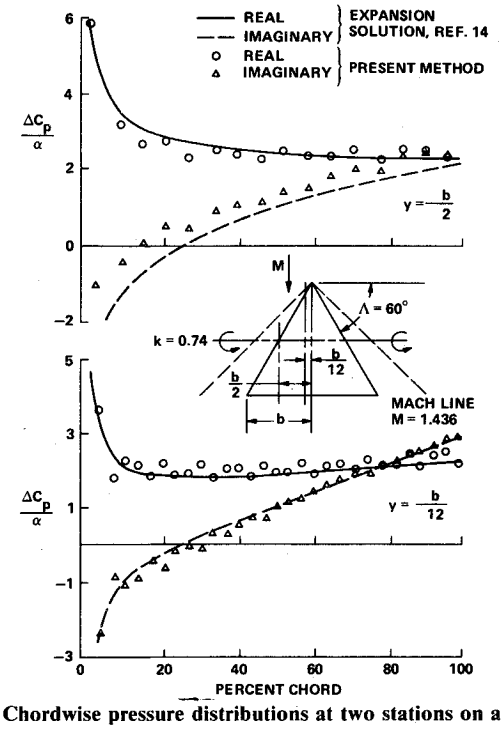


Fig. 9 Chordwise pressure distributions at two stations on a 60 deg swept delta wing oscillating in pitch.

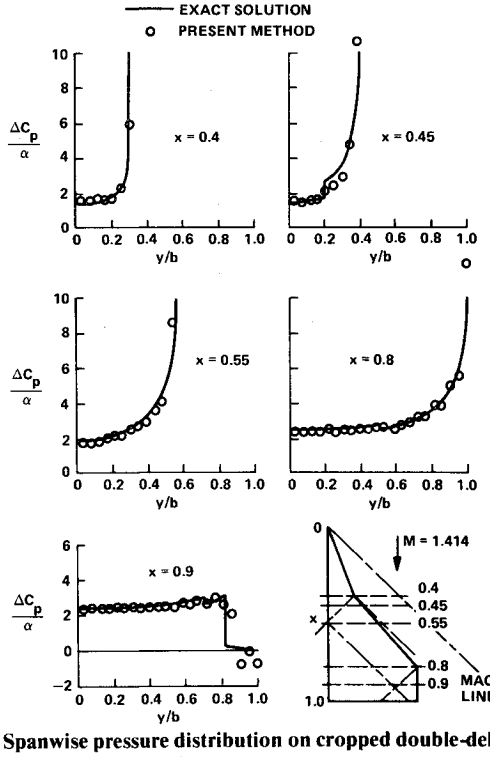


Fig. 10 Spanwise pressure distribution on cropped double-delta wing at steady-state angle of attack.

compares computed pressure at two spanwise stations with solutions from Ref. 14. Results compare favorably, although the imaginary part of the pressures calculated at the outboard station are predicting at a somewhat more forward center of pressure than is appropriate.

Computations also were performed on a more complex planform, namely, a cropped double-delta wing at a steady-state angle of attack at $M=1.414$. Resultant pressure distributions are compared in Fig. 10 with the exact solution of Ref. 15. Agreement is excellent except near the tip. Discontinuities are computed but are somewhat less pronounced than the exact theory predicts. In Fig. 11, the

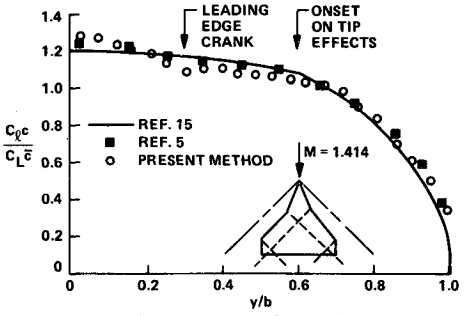


Fig. 11 Spanwise loading on cropped double-delta wing at steady-state angle of attack.

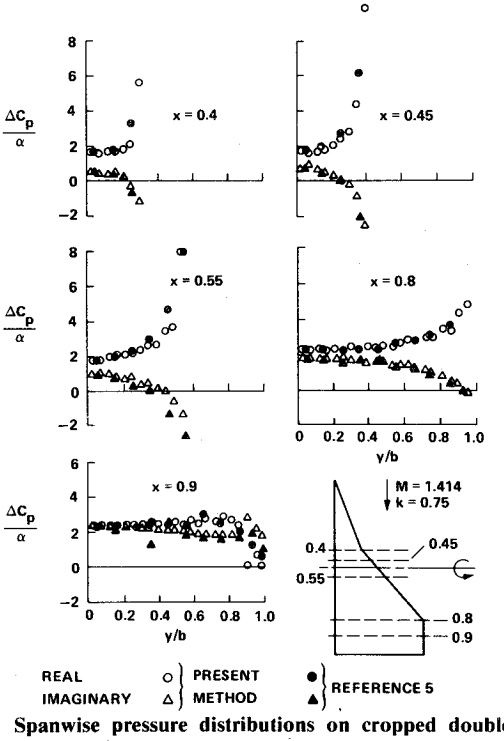


Fig. 12 Spanwise pressure distributions on cropped double-delta wing oscillating in pitch.

spanwise loading for this case is presented and compared with the exact solution and the finite-element solution of Ref. 5. Correlation is good, although the present method is slightly low in its lift prediction over the middle of the wing. It is interesting to note that both the present method and Ref. 5 predict a slope discontinuity caused by the leading-edge crank, as well as one caused by the tip effects, whereas Ref. 15 does not. Since such a discontinuity and a resultant higher lift on the inboard panel is physically logical, it would appear that Ref. 15 is in error.

In Fig. 12, pressures are shown for the same cropped double-delta wing oscillating in pitch about the root midchord at $k=0.75$. In the absence of an exact solution for this case, the comparisons are made with Ref. 5. Correlation is good except along the aftmost spanwise station ($x=0.9$). Since some irregularities in the solution for this station are acknowledged in Ref. 5, the accuracy of the present method cannot be assessed accurately here; however, the pressures from the Mach-box approach do appear well behaved here except at the very tip.

Finally, computations are presented in Fig. 13 for a swept rectangular wing at angle of attack. For the chosen combination of $M$, $\Lambda$, and $\mathcal{R}$, the wing has a subsonic trailing edge. Comparisons are made with theoretical pressure distributions from Ref. 13. Whereas correlation near the trailing edge is good for regions inboard of the tip Mach-line

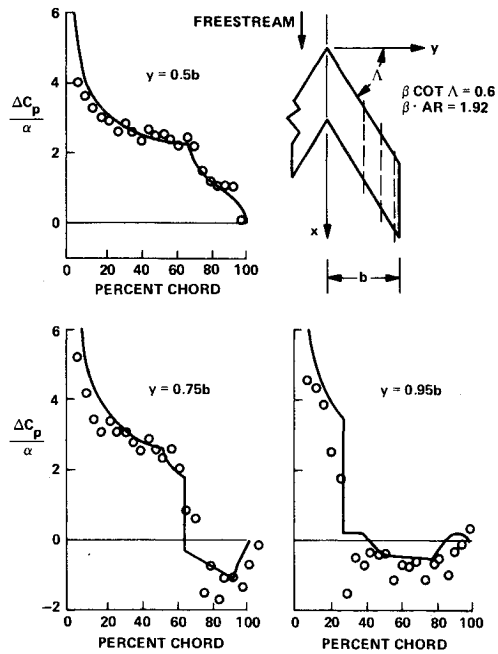


**Fig. 13 Chordwise pressure distributions for swept rectangular wing at steady-state angle of attack.**

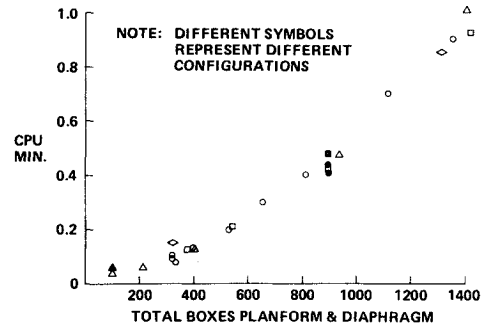


**Fig. 14 IBM 370/168 machine time as a function of number of boxes used in a Mach-box analysis for one Mach number and one reduced frequency.**

reflection, it noticeably worsens outboard of this. The program does appear to predict the discontinuities that occur in the outboard regions but is unable to capture properly the more detailed features of the pressure distribution there. Also, the program somewhat overpredicts the pressure reversal due to the tip effect.

To illustrate the computational efficiency of the method, CPU times for various analyses on the IBM 370/168 under the VS operating system were recorded. Figure 14 presents the results in the form of CPU time as a function of the total number of boxes, planform and diaphragm, used to perform the analyses of the various surfaces. Each point is for one Mach number and one reduced frequency; each different symbol is for a different type of wing. As can be seen, for any reasonable modeling, the time is under 1 min/calculation. For typical calculations on a simple planform (e.g., cropped delta or swept tapered), times of the order of 0.15 min are to be expected.

## Conclusions

The improvements to the Mach-box method of computing oscillatory aerodynamic influence coefficients presented in this paper result in realistic pressures that are much less erratic than those computed by the standard approach. Since the approach does not rely on function smoothing, it retains essential discontinuities in the pressure distributions. Furthermore, the method requires very little additional computer time and, hence, retains the cost-effectiveness of the standard Mach-box approach.

The method was applied to several standard test configurations, such as rectangular and delta wings both at a steady-state angle of attack and in oscillation. Correlation between computed pressures and lift distributions with available theoretical and other solutions was excellent in most cases. The method was shown to handle both subsonic and supersonic trailing edges correctly. Tip effects, however, seem to present some problems to the program on the more complex configurations. Reference 4 suggests that either a very fine grid be used near a side edge or that the square-root singularity of the diaphragm downwash near this tip be explicitly included in the formulation. This later refinement was shown in Ref. 16 to be successful for simple planforms when applied to a characteristic box formulation. Future incorporation of this refinement into the current approach is recommended, since it is our experience that simply using a finer grid is no solution for the problem.

## References

[1] Pines, S., Dujundji, J., and Neuringer, J., "Aerodynamic Flutter Derivatives for a Flexible Wing with Supersonic and Subsonic Edges," *Journal of Aeronautical Sciences*, Vol. 22, Oct. 1955, pp. 693-700.

[2] Watkins, C. E. and Berman, J. H., "On the Kernel Function of the Integral Equation Relating Lift and Downwash Distributions of Oscillating Wings in Supersonic Flow," NACA Rept. 1257, 1956.

[3] Cunningham, A. M. Jr., "Oscillatory Supersonic Kernel Function Methods for Interfering Surfaces," *Journal of Aircraft*, Vol. 11, Nov. 1974, pp. 664-670.

[4] Brock, B. J. and Griffin, J. A. Jr., "The Supersonic Doublet-Lattice Method – A Comparison of Two Approaches," AIAA Paper 75-760, Denver, Colo., May 1975.

[5] Giesing, J. P. and Kalman, T. P., "Oscillatory Supersonic Lifting Surface Theory Using a Finite Element Doublet Representation," AIAA Paper 75-761, Denver, Colo., May 1975.

[6] Bisplinghoff, R. L., Ashley, H., and Halfman, R. L., *Aeroelasticity*, Addison-Wesley, Cambridge, Mass., 1955, pp. 407-411.

[7] Evvard, J. C., "Distribution of Wave Drag and Lift in the Vicinity of Wing Tips at Supersonic Speeds," NACA TN 1382, 1947.

[8] Zartarian, G. and Zsu, P., "Theoretical Studies on the Prediction of Unsteady Supersonic Airloads on Elastic Wings," Wright Air Development Center, WADC TR 56-97, Pt. I, Dec. 1955, and Pt. II, Feb. 1956.

[9] Isaacson, E. and Keller, H. B., *Analysis of Numerical Methods*, Wiley, New York, 1966, pp. 327-335.

[10] Andrew, L. V. and Moore, M. T., "Further Developments on Supersonic Aerodynamic Influence Coefficient Methods," Proceedings of the AIAA Symposium on Structural Dynamics and Aeroelasticity, Aug. 1966.

[11] Ii, J. M., "Theoretical Studies to Refine the Prediction of Unsteady Aerodynamics of Supersonic Elastic Aircraft," Proceedings of AIAA Guidance, Control and Flight Mechanics Conference, Aug. 1970.

[12] Nelson, H. G., Rainey, R. A., and Watkins, C. E., "Lift and Moment Coefficients Expanded to the Seventh Power of Frequency for Oscillating Rectangular Wings in Supersonic Flow and Applied to a Specific Flutter Problem," NACA TN 3076, April 1954.

[13] Jones, R. T. and Cohen, D., *High Speed Wing Theory*, Princeton University Press, Princeton, N. J., 1960, pp. 191-236.

[14] Watkins, C. E. and Berman, J. H., "Air Forces and Moments on Triangular and Related Wings with Subsonic Leading Edges Oscillating in Supersonic Potential Flow," NACA TN-1099, 1952.

[15] Cohen, D. and Friedman, M. D., "Theoretical Investigation of the Supersonic Lift and Drag of Thin, Sweptback Wings with Increased Sweep Near the Root," NACA TN 2959, 1953.

[16] Stark, V. J. E., "Calculation of Aerodynamic Forces on Two Oscillating Finite Wings at Low Supersonic Mach Numbers," Saab TN 53, Linkoping, Sweden, 1964.

[17] Ii, J. M., Borland, C. J., and Hogley, J. R., "Prediction of Unsteady Aerodynamic Loading on Non-Planar Wings and Wing-Tail Configurations in Supersonic Flow," Air Force Flight Dynamics Lab., AFFDL-TR-71-108, Pt. 1, March 1972.

[18] Li, T., "Aerodynamic Influence Coefficients for an Oscillating Finite Thin Wing in Supersonic Flow," 23rd Annual Institute of Aerospace Sciences Meeting, Jan. 1955.